Journal of Molecular Structure 1235 (2021) 130226

Contents lists available at ScienceDirect

Journal of Molecular Structure

journal homepage: www.elsevier.com/locate/molstr

Levofloxacin and sulfa drugs linked via Schiff bases: Exploring their urease inhibition, enzyme kinetics and *in silico* studies

Syed Azhar Ali Shah Tirmazi[a], Muhammad Abdul Qadir[a], Mahmood Ahmed[b,c,*], Muhammad Imran[d], Riaz Hussain[e], Mehwish Sharif[a], Muhammad Yousaf[f], Muhammad Muddassar[g,*]

[a] Institute of Chemistry, University of the Punjab. Lahore 54590, Pakistan
[b] Renacon Pharma Limited, Lahore 54600, Pakistan
[c] Division of Science and Technology, University of Education, Lahore, Pakistan
[d] KAM School of Life Sciences, FC College (A Chartered University), Lahore, Pakistan
[e] Department of Chemistry, University of Okara, Okara, Pakistan
[f] Department of Chemistry and Biology, Ryerson University, 350 Victoria Street Toronto Ontario, M5B 2K3 Canada
[g] Department of Biosciences, COMSATS University Islamabad, Park Road, Islamabad, Pakistan

ARTICLE INFO

Article history:
Received 10 August 2020
Revised 5 January 2021
Accepted 26 February 2021
Available online 6 March 2021

Keywords:
Levofloxacin
Sulfonamides
Urease
Docking studies
DFT

ABSTRACT

Involvement of urease in various pathological conditions specifically in gastric and peptic ulcers make it an important therapeutic target. In the present study urease inhibition was investigated by newly designed Schiff bases of levofloxacin. Structure elucidation of these compounds were done by spectral studies such as IR, ^{1}H NMR and ^{13}C NMR and elemental analysis. In vitro urease enzyme inhibition assay revealed the compounds LS01, LS06 and LS07 were found to be the most potent and showed comparable IC_{50} values 0.58±0.11, 0.45±0.21 μM and 0.52±0.28 μM respectively. The compound LS06 was competitive inhibitor with Ki value 1.13 μM while the compounds LS01 and LS07 were mixed type of inhibitors with Ki values 3.40 and 6.03 μM respectively. Plausible binding mode of competitive inhibitor was predicted using molecular docking studies. Ancillary to synthetic studies, density functional theory (DFT) at B3LYP/6–31G(d,p) basis sets in ground state is utilized in order to gain optimized geometries of LS01-LS09 molecules. Different geometric parameters like molecular electrostatic potential analysis, alignment of HOMO and LUMO levels, natural bonding orbital (NBO) analysis and global descriptor of reactivity were performed in support of experimental findings. All DFT based computed results showed best agreement with experimental finding and suggest that all synthesized compounds are chemically stable.

1. Introduction

Urease also known as urea amidohydrolase is a metal containing enzyme that catalyzes the hydrolysis of urea producing ammonia and carbon dioxide. It is ubiquitously found in diverse varieties of organisms including plant, fungi and algae [1,2]. Urease producing bacteria cause an adverse effect on human health. Urease contributes a major part in the diseases caused by *Helicobacter pylori* (*H. pylori*). These bacteria sustain at low pH during colonization causing gastric and peptic ulcers, in occasional cases these may cause cancer [3]. For colonization of bacterium in *H. pylori* infection, urease activity is indispensable as urease knockout bacteria losing their ability to establish infection. *H. pylori* depends on urease activity for bacterial sustainability at low pH in the stomach, consequently a bacterium can be exterminated at early stages of infection by focusing on urease activity [4,5]. The structure, molecular weight and amino acid sequence of urease are highly dependent on its source. The bacterial ureases are heteropolymeric molecules consisted of three different subunits; α, β and γ while the jack bean ureases are homohexameric molecules consisted of six α subunits only. Nevertheless, the active site of the enzyme is mainly conserved despite the dissimilarity in the structure of both ureases because the active site is always located on α subunits consisting of binuclear nickel center [6,7]. Designing of novel urease inhibitors is of main research interest due to the association of urease with bacterial infections. Current availability of urease inhibitors is very limited. Nevertheless, different classes of in-

* Corresponding author at: Division of Science and Technology, University of Education, Lahore, Pakistan.
E-mail addresses: mahmoodresearchscholar@gmail.com (M. Ahmed), mmuddassar@comsats.edu.pk (M. Muddassar).

https://doi.org/10.1016/j.molstruc.2021.130226
0022-2860/

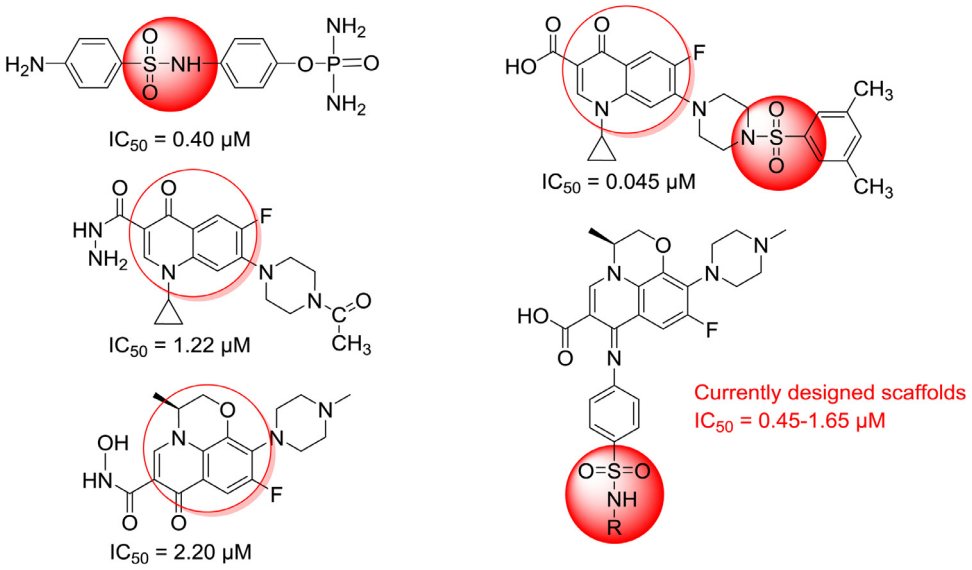

Fig. 1. Literature reported and currently designed scaffolds as urease inhibitors.

hibitors are available in literature that include phosphate derivatives (phenylphosphorodiamidates, phosphorotriamides, phosphorylamides) [8], barbituric acid analogues [9], thiourea derivatives [10], five and six-membered heterocyclics, natural products and metal complexes [11]. The structures of some good urease inhibitors previously reported are presented in Fig. 1. Schiff bases are compounds that contain a special group called imine or azomethine (-CH = *N*) having carbon nitrogen double bond and are synthesized by reaction of primary amine and carbonyl compounds. Schiff bases are very important in both medicine as well as pharmaceutical industry due to wide variety of biological activities like antibacterial, antifungal, antiviral, antiproliferative, antipyretic, antimalarial and anti-inflammatory properties [12,13]. The biological properties of Schiff bases are attributed to the presence of lone pair of electrons present on imine group that can be easily donated [14,15]. Similarly sulfonamides have also shown pharmacological properties against various therapeutic targets those are from antibacterial to anticancer [16,17]. Urease inhibition by sulfonamides [18,19] and Schiff bases [20-24] have been reported in literature. Levofloxacin belongs to fluoroquinolone class of antibiotics that is active against plentiful bacterial infections including urinary tract, gastrointestinal tract and respiratory infections [25]. It was also reported that levofloxacin exhibited excellent urease inhibitory activities [26]. In recent era high level of resistance shown by *H. pylori* against antibiotics and the reduced patient acquiescence demands new inhibitors with enhanced efficacy and simple treatment [27,28]. The work presented herein is directed towards microwave assisted synthesis of Schiff bases of levofloxacin with different sulfa drugs. Microwave assisted synthesis is economical moreover it is environmental friendly, time saving and cost effective. To the best of our knowledge, this is a first report on levofloxacin conjugated with sulfa drugs as inhibitors of urease enzyme. Due to the involvement of ureases in different pathological conditions, the discovery of safe and potent urease inhibitors has been an area of challenge in pharmaceutical research. Also, enzyme kinetics and molecular modeling studies were performed to have insight into detailed inhibition mechanism and binding conformation of competitive inhibitor in urease enzyme. To date, there is no density functional theory carried out on these compounds. So, we performed various DFT based calculations like, molecular electrostatic potential analysis, natural bonding orbital analysis, global descriptor of reactivity and frontier molecular orbital analysis for estimating the different reactive sights and stability of newly designed molecules.

2. Experimental

Newly designed Schiff bases were synthesized by using high purity chemicals originate to Sigma Aldrich, USA, which were purchased from Hajvery Chemicals, Lahore-Pakistan whereas Milli-Q® water system (UK) was employed for high purity water production. Structure elucidation of compounds were done by spectral studies such as IR (FTIR spectrophotometer, Bruker Technologies, USA), ^{1}HNMR-500 MHz, ^{13}CNMR-125 MHz (NMR spectrometer, Bruker, USA). Elemental analysis (C, H, N and S) was done by HT+ elemental analyser by Thermo Scientific, UK). Gallenkamp apparatus was employed for determination of melting point while for TLC analysis, pre-coated silica plates (Merck, Germany) were spotted and purity of synthesized compounds was confirmed in UV light.

2.1. Synthesis protocol for schiff bases (LS01-LS09)

In a 100 mL round bottom flask, levofloxacin (1 mmol, 1 eq.) and respective sulfonamides (1 mmol, 1 eq.) were dissolved in boiling methanol (20 mL). Then glacial acetic acid (0.5 mL) was added as a catalyst. The reaction mixture was refluxed in a microwave oven at medium high power (500 W) till the completion of reaction (2 hrs). The progress of reaction was monitored by TLC using dichloromethane: methanol: ammonia as solvent mixture in 75: 25: 1 ratio till the appearance of single spot. After total consumption of reactants, the contents were cooled; precipitates were collected and finally washed with cold methanol to get the desired product. Purification was achieved by passage of dissolved product through a short column with silica gel packing and dichloromethane: methanol (75: 25) as solvent system. Details chemistry for synthesis of compounds LS01-LS09 explained below.

2.1.1. (S)−7-((4-(N-(3,4-dimethylisoxazol-5-yl)sulfamoyl)phenyl)imino)−9-fluoro-3-methyl-10-(4-methylpiperazin-1-yl)−2,3-dihydro-7H-[1,4]oxazino[2,3,4-ij]quinoline-6-carboxylic acid (LS01)

Appearance, Pale yellow solid; Yield, 85.73%; M.P., 228 °C; Rf, 0.70; IR (ATR, υ cm^{-1}): 3420 (sulfonyl-NH), 3254 (carboxylic-OH), 2919 (=*C*–H), 2851 (-C-H), 1648 (imine –CH=*N*-), 1596 (–CH–CH,

stretch aromatic), 1454 (-C_6H_5), 1363 (-NH-*S* = *O* asymmetric stretch), 1149.30 (–SO_2-NH symmetric stretch), 1299, 1197 (C–N stretch), 1088.01 (-*S* = *O*), 1049 (Ar-C-F); ^{1}H NMR (400 MHz, DMSO–d_6): δ_H (ppm) 11.38 (1H, s, -OH), 10.08 (1H, s, N–H), 8.88 (1H, s, =CH–N), 7.51 (2H, d, *J* = 8.6 Hz, ArH-), 7.46 (2H, d, *J* = 7.6 Hz, ArH-), 6.48 (2H, s, =CH-), 4.88 (1H, s, –CH–CH_3), 4.40 (2H, d, *J* = 8, -O-CH_2), 3.27 (4H, t, *J* = 8 Hz, N–CH_2), 2.46 (4H, t, *J* = 3.6 Hz, N–CH_2), 2.22 (3H, s, N–CH_3), 2.00 (3H, s, CH_3), 1.85 (3H, s, CH_3), 1.42 (3H, s, CH_3); ^{13}C NMR (100 MHz, DMSO–d_6): δ (ppm) 174.10, 174.13, 164, 157, 156, 155, 154, 144, 140.62, 140.52, 131.40, 131.25, 124, 122.10, 122.01, 110, 103.85, 103.65, 68, 55, 54, 50.59, 50.56, 46, 22, 18, 16; Anal. Calc. for $C_{29}H_{31}FN_6O_6S$ (FW = 610.65 g/mol): C, 57.04; H, 5.12; N, 13.76; S, 5.25%; Found: C, 57.18; H, 5.26; N, 13.67; S, 5.38%.

*2.1.2. (S)–9-fluoro-3-methyl-10-(4-methylpiperazin-1-yl)–7-((4-(N-(thiazol-2-yl)sulfamoyl)phenyl)imino)–2,3-dihydro-7H-[1,4]oxazino[2,3,4-*ij*]quinoline-6-carboxylic acid (LS02)*

Appearance, Yellow solid; Yield, 86.78%; M.P., 252 °C; Rf, 0.72; IR (ATR, υ cm^{-1}): 3477.21 (sulfonyl-NH), 3309.06 (carboxylic-OH), 2931.87 (=*C*–H), 2811.96 (-C-H), 1646.27 cm^{-1} (imine –CH=*N*-), 1593.74 (–CH–CH stretch aromatic), 1445.67 (-C_6H_5), 1380.10 (-NH-*S* = *O* asymmetric stretch),1132.08 (–SO_2-NH symmetric Stretch), 1287.75, 1235.56 (C–N stretch), 1075.23 (-*S* = *O*), 1049.67 (Ar-C-F); ^{1}H NMR (400 MHz, DMSO–d_6): δ_H (ppm) 11.38 (1H, s, -OH), 10.62 (1H, s, -NH), 8.95 (1H, s, =CH–N), 8.76 (6H, m, =CH), 7.48 (1H, s, =CH), 4.86 (1H, s, –CH–CH_3), 4.44 (2H, d, *J* = 8 Hz, -O-CH_2), 3.27 (4H, d, *J* = 3.6, N–CH_2), 2.46 (4H, d, *J* = 3.2 Hz, N–CH_2), 2.22 (3H, s, N–CH_3), 1.41 (3H, s, CH_3); ^{13}C NMR (100 MHz, DMSO–d_6): δ (ppm) 174.13, 174.10, 166, 164, 156, 154, 144, 140.62, 140.55, 135, 131.42, 131.25, 124, 122.10, 122.01, 116, 103.85, 103.65, 68, 55, 54, 50.59, 50.56, 46, 18; Anal. Calc. for $C_{27}H_{27}FN_6O_5S_2$ (FW = 598.67 g/mol): C, 54.17; H, 4.55; N, 14.04; S, 10.71%; Found: C, 54.24; H, 4.68; N, 14.0; S, 10.84%.

*2.1.3. (S)–9-fluoro-3-methyl-10-(4-methylpiperazin-1-yl)–7-((4-(N-(pyrimidin-2-yl)sulfamoyl)phenyl)imino)–2,3-dihydro-7H-[1,4]oxazino[2,3,4-*ij*]quinoline-6-carboxylic acid (LS03)*

Appearance, Yellow solid; Yield, 75.04%; M.P., 180 °C; Rf, 0.75; IR (ATR, υ cm^{-1}): 3497.67 (sulfonyl-NH), 3309.63 (carboxylic-OH), 2937.83 (=*C*–H), 2850.49 (-C-H), 1650.73 (imine –CH=*N*-), 1596.22 (–CH–CH stretch aromatic), 1449.47 (-C_6H_5), 1380.88 (-NH-*S* = *O* asymmetric stretch), 1134.74 (–SO_2-NH symmetric Stretch), 1290.70, 1239.00 (C–N stretch), 1078.00 (-*S* = *O*), 1045.68 (Ar-C-F); ^{1}H NMR (400 MHz, DMSO–d_6): δ_H (ppm) 11.39 (1H, s, -OH), 10.59 (1H, s, -NH), 8.75 (2H, s, =CH–N), 8.55 (1H, s, =CH–N), 7.49 (4H, *d* = 8 Hz, =CH aromatic), 4.82 (1H, s, –CH–CH_3), 4.42 (2H, d, *J* = 8 Hz, -O-CH_2), 3.30 (4H, d, *J* = 3.6 Hz, N–CH_2), 2.46 (4H, d, *J* = 3.2 Hz, N–CH_2), 2.22 (3H, s, N–CH_3), 1.41 (3H, s, CH_3); ^{13}C NMR (100 MHz, DMSO–d_6): δ (ppm) 174.13, 174.10, 164, 156, 154, 144, 140.62, 140.55, 131.41, 131.27, 124, 122.11, 122.02, 110, 103.85, 103.65, 68, 55, 54, 50.59, 50.56, 46, 18; Anal. Calc. for $C_{28}H_{28}FN_7O_5S$ (FW = 593.63 g/mol): C, 56.65; H, 4.75; N, 16.52; S, 5.40%; Found: C, 56.55; H, 4.68; N, 16.68; S, 5.51%.

*2.1.4. (S)–9-fluoro-3-methyl-10-(4-methylpiperazin-1-yl)–7-((4-(N-(4-methylpyrimidin-2-yl)sulfamoyl)phenyl)imino)–2,3-dihydro-7H-[1,4]oxazino[2,3,4-*ij*]quinoline-6-carboxylic acid (LS04)*

Appearance, Pale yellow solid; Yield, 78.91%; M.P., 192 °C; Rf, 0.74; IR (ATR, υ cm^{-1}): 3493.87 (sulfonyl-NH), 3305.66 (carboxylic-OH), 2937.54 (=*C*–H), 2846.68 (-C-H), 1648.25 (imine –CH=*N*-), 1594.01 (–CH–CH stretch aromatic), 1446.85 (-C_6H_5), 1379.08 (-NH-*S* = *O* asymmetric stretch), 1132.71 (–SO_2-NH symmetric stretch), 1288.64, 1236.92 (C–N stretch), 1075.40 (-*S* = *O*), 1043.97 (Ar-C-F); ^{1}H NMR (400 MHz, DMSO–d_6): δ_H (ppm) 11. 38 (1H, s, -OH), 10.60 (1H, s, -NH), 8.95 (1H, s, =CH–N), 8.75 (2H, s, =CH–N), 7.50–7.48 (5H, m, =CH), 4.80 (1H, s, –CH–CH_3), 4.44 (2H, d, *J* = 8 Hz, -O-CH_2), 3.30 (4H, d, *J* = 4.4 Hz, N–CH_2), 2.46 (4H, d, *J* = 3.2 Hz, N–CH_2), 2.20 (6H, s, N–CH_3), 1.42 (3H, s, CH_3); ^{13}C NMR (100 MHz, DMSO–d_6):δ (ppm) 174.13, 174.10, 164, 156, 154, 144, 140.62, 140.55, 131.40, 131.25, 124, 122.10, 122.01, 110, 103.85, 103.65, 68, 55, 54, 50.59, 50.56, 46, 18.38, 18.36; Anal. Calc. for $C_{29}H_{30}FN_7O_5S$ (FW = 607.66 g/mol): C, 57.32; H, 4.98; N, 16.14; S, 5.28%; Found: C, 57.44; H, 4.91; N, 16.28; S, 5.39%.

*2.1.5. (S)–7-((4-(N-(4,6-dimethylpyrimidin-2-yl)sulfamoyl)phenyl)imino)–9-fluoro-3-methyl-10-(4-methylpiperazin-1-yl)–2,3-dihydro-7H-[1,4]oxazino[2,3,4-*ij*]quinoline-6-carboxylic acid (LS05)*

Appearance, Brownish yellow solid; Yield, 86.63%; M.P., 114 °C; Rf, 0.69; IR (ATR, υ cm^{-1}): 3490.20 (sulfonyl-NH), 3269.12 (carboxylic-OH), 2921.04 (=*C*–H), 2839.98 (-C-H), 1649.17 (imine –CH=*N*-), 1588.37 (–CH–CH stretch aromatic), 1459.23 (-C_6H_5), 1369.77 (-NH-*S* = *O* asymmetric stretch), 1132.93 (–SO_2-NH symmetric stretch), 1289.28, 1224.10 (C–N stretch), 1074.62 (-*S* = *O*), 1044.23 (Ar-C-F).; ^{1}H NMR (400 MHz, DMSO–d_6): δ_H (ppm) 11.38 (1H, s, -OH), 10.60 (1H, s, -NH), 8.74 (1H, s, =CH), 7.52–7.48 (5H, m, =CH), 4.83 (1H, s, –CH–CH_3), 4.44 (2H, d, *J* = 8 Hz, -O-CH_2), 3.31 (4H, d, *J* = 2.8 Hz, N–CH_2), 2.48 (4H, d, *J* = 2.4 Hz, N–CH_2), 2.45 (6H, s, CH_3), 2.27 (3H, s, N–CH_3), 1.41 (3H, s, CH_3); ^{13}C NMR (100 MHz, DMSO–d_6): δ (ppm) 174.13, 174.10, 164, 156, 154, 152, 144, 140.62, 140.55, 131.40, 131.25, 124, 122.10, 122.02, 110, 103.85, 103.65, 68, 55, 54, 50.59, 50.56, 46, 22, 18; Anal. Calc. for $C_{30}H_{32}FN_7O_5S$ (FW = 621.68 g/mol): C, 57.96; H, 5.19; N, 15.77; S, 5.16%; Found: C, 58.06; H, 5.31; N, 15.6; S, 5.24%

*2.1.6. (3S)–7-[(4-{[(5,6-*dimethoxypyrimidin-4-yl)amino*]sulfonyl}phenyl)imino]–9-fluoro-3-methyl-10-(4-methylpiperazin-1-yl)–2,3-dihydro-7*H*-[1,4]oxazino[2,3,4-*ij*]quinoline-6-carboxylic acid (LS06)*

Appearance, Pale yellow solid; Yield, 75.80%; M.P., 278 °C; Rf, 0.68; IR (ATR, υ cm^{-1}): 3446.69 (sulfonyl-NH), 3301.00 (carboxylic-OH), 2933.34 (=*C*–H), 2832.49 (-C-H), 1649.59 (imine –CH=*N*-), 1596.66 (–CH–CH stretch aromatic), 1450.91 (-C_6H_5), 1382.44 (-NH-*S* = *O* asymmetric stretch), 1134.64 (–SO_2-NH symmetric stretch), 1289.31, 1237.49 (C–N stretch), 1078.96 (-*S* = *O*), 1045.41 (Ar-C-F); ^{1}H NMR (400 MHz, DMSO–d_6): δ_H (ppm) 11.38 (1H, s, -OH), 10.62 (1H, s, -NH), 8.95 (1H, s, N–H), 8.76 (1H, s, =CH–C), 7.50–7.48 (5H, m, =CH), 4.86 (1H, s, –CH–CH_3), 4.44 (2H, d, *J* = 8 Hz, -O-CH_2), 3.98 (3H, s, 1 x OCH_3), 3.82 (3H, s, 1 x OCH_3), 3.28 (4H, d, *J* = 3.6 Hz, N–CH_2), 2.46 (4H, d, *J* = 3.2 Hz, N–CH_2), 2.22 (3H, s, N–CH_3), 1.41 (3H, s, CH_3); ^{13}C NMR (100 MHz, DMSO–d_6): δ (ppm) 174.13, 174.10, 164, 156, 154, 152, 150, 147, 144, 140.62, 140.55, 131.40, 131.25, 124, 122.10, 122.02, 103.85, 103.65, 68, 55, 54 (OCH_3 x 2), 52, 50, 46, 18; Anal. Calc. for $C_{30}H_{32}FN_7O_7S$ (FW = 653.68 g/mol): C, 55.12; H, 4.93; N, 15.00; S, 4.90%; Found: C, 55.28; H, 4.98; N, 15.16; S, 4.82%.

*2.1.7. (S)–7-((4-(N-acetylsulfamoyl)phenyl)imino)–9-fluoro-3-methyl-10-(4-methylpiperazin-1-yl)–2,3-dihydro-7H-[1,4]oxazino[2,3,4-*ij*]quinoline-6-carboxylic acid (LS07)*

Appearance, Pale yellow solid; Yield, 73.60%; M.P., 118 °C; Rf, 0.78; IR (ATR, υ cm^{-1}): 3494.72 (sulfonyl-NH), 3318.35 (carboxylic-OH), 2935.55 (=*C*–H), 2846.67 (-C-H), 1651.03 (imine –CH =*N*-), 1595.46 (–CH–CH stretch aromatic), 1448.44 (-C_6H_5), 1378.91 (-NH-*S* = *O* asymmetric stretch), 1134.72 (–SO_2-NH symmetric stretch),1290.95, 1238.39 (C–N stretch), 1077.52 (-*S* = *O*), 1045.39 (Ar-C-F); ^{1}H NMR

(400 MHz, DMSO–d_6): δ_H (ppm) 11.40 (1H, s, -OH), 10.60 (1H, s, -NH), 8.88 (1H, s, =CH–N), 8.75 (1H, s, =CH), 7.45–7.42 (4H, m, =CH), 4.84 (1H, s, –CH–CH_3), 4.44 (2H, d, J = 8 Hz, -O-CH_2), 3.25 (4H, d, J = 3.6 Hz, N–CH_2), 2.50 (4H, d, J = 3.2 Hz, N–CH_2), 2.42 (3H, s, N–CH_3), 2.24 (3H, s, $O = C$–CH_3), 1.42 (3H, s, CH_3); ^{13}C NMR (100 MHz, DMSO–d_6): δ (ppm) 176, 174, 166, 164, 156, 154, 152, 146, 144, 140, 131, 130, 127, 125, 124, 122, 121, 112, 110, 103, 68, 55, 54, 50, 46, 18; Anal. Calc. for $C_{26}H_{28}FN_5O_6S$ (FW = 557.60 g/mol): C, 56.01; H, 5.06; N, 12.56; S, 5.75%; Found: C, 56.35; H, 5.31; N, 12.35; S, 5.84%.

2.1.8. (S)–7-((4-(N-carbamimidoylsulfamoyl)phenyl)imino)–9-fluoro-3-methyl-10-(4-methylpiperazin-1-yl)–2,3-dihydro-7H-[1,4]oxazino[2,3,4-ij]quinoline-6-carboxylic acid (LS08)

Appearance, Dark brown solid; Yield, 82.94%; M.P., 298 °C; Rf, 0.77; IR (ATR, υ cm^{-1}): 3392.45 (sulfonyl-NH), 3214.32 (carboxylic-OH), 1611.97 (imine –CH =N-), 1524.93 (–CH–CH $_{\text{stretch (aromatic}}$), 1496.10 (-$C_6H_5$), 1305.25 (-NH-$S = O$ $_{\text{asymmetric stretch}}$), 1123.92 (–$SO_2$–NH $_{\text{symmetric stretch}}$), 1229.40, 1174.20 (C–N $_{\text{stretch}}$), 1081.46 (-$S = O$), 1050.56 (Ar-C-F); ^{1}H NMR (400 MHz, DMSO–d_6): δ_H (ppm) 11.39 (1H, s, COOH), 10.64 (1H, s, =CH–N), 8.75 (1H, s, = CH–C), 7.49 (4H, d, J = 8 Hz, = CH), 5.25 (2H, s, NH_2), 4.85 (1H, s, –CH–CH_3), 4.45 (2H, d, J = 8 Hz, -O-CH_2), 3.30 (4H, d, J = 3.6 Hz, N–CH_2), 2.44 (4H, d, J = 3.2 Hz, N–CH_2), 2.25 (3H, s, N–CH_3), 1.44 (3H, s, -CH_3); ^{13}C NMR (100 MHz, DMSO–d_6): δ (ppm) 174, 166, 164, 156, 154, 144, 140.65, 140.56, 131.40, 131.25, 124, 122.10, 122.02, 110, 103.90, 103.66, 68, 55, 54, 50.61, 50.57, 46, 18; Anal. Calc. for $C_{25}H_{28}FN_7O_5S$ (FW = 557.60 g/mol): C, 53.85; H, 5.06; N, 17.58; S, 5.75%; Found: C, 53.92; H, 5.10; N, 17.75; S, 5.88%.

2.1.9. (S)–9-fluoro-3-methyl-10-(4-methylpiperazin-1-yl)–7-((4-sulfamoylphenyl)imino)–2,3-dihydro-7H-[1,4]oxazino[2,3,4-ij]quinoline-6-carboxylic acid (LS09)

Appearance, Bright yellow solid; Yield, 80.00%; M.P., 286 °C; Rf, 0.80; IR (ATR, υ cm^{-1}): 3499.14 (sulfonyl-NH), 3300.00 (carboxylic-OH), 2938.47 (=C–H), 2849.88 (-C-H), 1650.32 (imine –CH =N-), 1594.49 (–CH–CH $_{\text{stretch aromatic}}$), 1448.64 (-$C_6H_5$), 1378.02 (-NH-$S = O$ $_{\text{asymmetric stretch}}$), 1134.49 (–$SO_2$–NH $_{\text{symmetric stretch}}$), 1290.67, 1238.28 (C–N $_{\text{stretch}}$), 1077.04 (-$S = O$), 1045.60 (Ar-C-F); ^{1}H NMR (400 MHz, DMSO–d_6): δ_H (ppm) 11.38 (1H, s, COOH), 10.62 (1H, s, =CH–N), 8.95 (2H, s, NH_2), 8.76 (1H, s, =CH–C), 7.49 (4H, d, J = 8 Hz, =CH), 4.86 (1H, s, –CH–CH_3), 4.44 (2H, d, J = 8 Hz, -O-CH_2), 3.28 (4H, d, J = 3.6 Hz, N–CH_2), 2.46 (4H, d, J = 3.2 Hz, N–CH_2), 2.22 (3H, s, N–CH_3), 1.41 (3H, s, CH_3); ^{13}C NMR (100 MHz, DMSO–d_6): δ (ppm) 174, 164, 156, 154, 144, 140.65, 140.56, 131.41, 131.27, 124, 122.11, 122.03, 110, 103.90, 103.66, 68, 55, 54, 50.61, 50.57, 46, 18; Anal. Calc. for $C_{24}H_{26}FN_5O_5S$ (FW = 515.56 g/mol): C, 55.91; H, 5.08; N, 13.58; S, 6.22%; Found: C, 55.82; H, 5.19; N, 13.71; S, 6.11%.

2.2. Antiurease assay

Urease inhibition assay was performed as reported in our earlier studies [24,29,30]. Briefly, the inhibitors (synthesized compounds) and thiourea (positive control) were dissolved in DMSO. Aliquots of 250–0.49 μM of inhibitors (triplicate), 10 μL phosphate buffer (K_2HPO_4, pH = 6.8–7.0, 50 mmol), 20 μL of jack bean urease (UNI-CHEM, U30550–2E) were incubated at 37 °C for 10 min. 20 mM substrate (40 μL, urea) was added in each well and incubated for 10 min. at same temperature. Subsequently, phenol reagent (40 μL) and alkali reagent (40 μL) containing 0.1% active chlorine was added to each well and placed for 50 min. at room temperature. Percentage urease inhibition was determined by using below equation after measuring the absorbance of each well at 625 nm by employing the Labtech, LT-4500 (UK) micro plate reader.

$$\%\,\text{Urease inhibition} = \{1 - T/C\} \times 100$$

Where, T is absorbance of each well containing inhibitor while C is absorbance of blank and results are presented as mean±SEM.

IC_{50} values of each inhibitor was calculated by regression equation where 50% inhibition was observed. For kinetics studies, binding mechanism of each inhibitor was carried out at different concentrations (0–20 μM). These five different inhibitor concentrations were reacted with different concentration of substrate (urea, 0.5–4.0 mM) to evaluate whether the inhibitors showed inhibition behavior in competitive, non-competitive (mixed) or uncompetitive way. Primary and secondary Lineweaver Burk plots were drawn to determine the $K_{m\,(app)}$, $V_{max\,(app)}$ and K_i (inhibition constant) respectively by using GraphPad PRISM 7.0.

2.3. Molecular docking studies

2.3.1. Protein structure and newly synthesized compounds preparation

Jack bean urease (PDB ID 4H9M) X-rays structure was downloaded from protein data bank (PDB) (https://www.rcsb.org/). The missing hydrogen atoms and side chains were added using Schrodinger software “protein preparation wizard” utility. All the cocrystal ligands and crystalized buffer reagents were removed except the Ni ions present at the catalytic site. Protein structure was energy minimized to relieve the steric hindrance among the residues by using OPLS2005 force field. During minimization, the structure was allowed to deviate 0.3 Å from its X-rays conformation. Then synthesized compounds were sketched using maestro “Build” toolbar. The LigPrep tool implemented in Schrodinger software was used to generate possible ionization states and different conformations of the compound.

2.3.2. Grid generation and docking protocol

Before docking the competitive inhibitor in the catalytic site of urease enzyme, Grid box was generated by setting the size of cubic box 20 Å in each dimension. X, Y, Z coordinates (17.5, 36.56, 20.48) were selected as center of the grid box. All other parameters like cutoff radius scaling and van der Waals factor were used with their default values. Then prepared competitive inhibitor was docked into the urease enzyme grid using GLIDE software. The standard precision mode (SP) was used to identify best plausible binding pose. During docking 200 conformations were generated in the active site, out of which top five were minimized in binding site and eventually best pose was selected based on the docking score.

2.4. Computational studies

Gaussian 09 program package [31] was employed for the DFT calculations of investigated compounds LS01-LS09. B3LYP method combined with 6–31 G(d,p) basis set of density functional theory without symmetry restriction is applied on all the compound for gaining optimized geometries. NBO 3.1 package is applied for natural bonding orbital analysis at same basis set for investigating different transitions. Alignment of frontier molecular orbitals, global indices of reactivity and molecular electrostatic potential analysis was conducted at B3LYP/6–31 G(d,p) for LS01-LS09 compounds in order to check the stability factor associated with DFT based optimized geometries. Gauss View 5 [32] served for input files designing and interpreting of output results were done by employing Avogadro and Chemcraft programs [33,34].

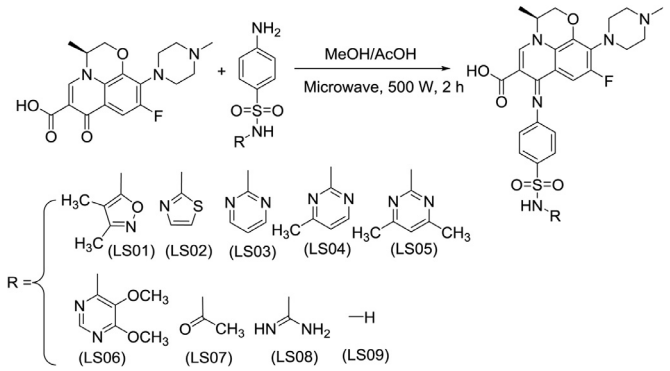

Scheme 1. Synthesis of Schiff bases.

3. Results and discussion

3.1. Chemistry

The target Schiff bases of levofloxacin with sulfonamide moiety were prepared by interaction of levofloxacin with sulfa drugs such as sulfafurazole, sulfathiazole, sulfadiazine, sulfamerazine, sulfadimidine, sulfadoxine, sulfacetamide, sulfaguanidine and sulfanilamide. The sulfonamide molecules have been attached to ketonic group of levofloxacin using methanol as solvent and acetic acid as catalyst in the synthesis of Schiff bases LS01-LS09. The Schiff bases were obtained in good yield (73.6–92.5%). Synthetic route and structures of Schiff bases are represented in Scheme 1. All the synthesized compounds were characterized by performing IR, ^{1}H NMR and ^{13}C NMR spectral studies. In the IR spectra of Schiff bases (LS01-LS09), the broad band appeared in range of 3392.45–3499.14 cm^{-1} indicating the presence of N–H moiety of sulfonamides. The broad band appeared at 3214.32–3318.35 cm^{-1} represented the carboxylic OH group. The peak between 2919.39–2938.47 cm^{-1} represented = *C*–H stretching whereas peaks at 2811.96–2851.65 cm^{-1} represented C–H stretching and a sharp band at 1705.15 cm^{-1} presented *C = O*. When the Schiff base was formed that band of keto group disappeared while a very strong band between 1611.97 - 1651.03 cm^{-1} was obtained which confirmed the imine (*-C = N*) formation. The band appeared at 1524.93–1596.69 cm^{-1} represented the -CH–CH- stretch (aromatic). The broad band at 1445.67–1496.10 cm^{-1} indicated the presence of aromatic ring. A band at 1305.25–1382.44 cm^{-1} indicated the presence of $-SO_2$-NH (asymmetric stretch) while a sharp band at 1123.92–1149.30 cm^{-1} confirmed $-SO_2$-NH (symmetric stretch) of sulfonamide. The peaks for C–N stretch were obtained at 1174.20–1299.72 cm^{-1}. The peak for *S = O* of sulfonamide was obtained between 1074.62–1088.01 cm^{-1} while the peak for Ar-C-F of levofloxacin was obtained between 1043.97–1050.56 cm^{-1}. In ^{1}H NMR spectra, Schiff bases (LS01-LS09) exhibited broad singlet between δ 8.95 - 8.54 and 5.25 ppm assigned to proton of N–H of sulfonamides. The singlet at δ 2.27 - 2.20 ppm was assigned to proton of CH_3 group attached to piperazine moiety while singlet at δ 1.42–1.40 ppm was assigned to proton of CH_3 group linked to morpholine moiety. In conjugate LS01, the singlets at δ 2.00 and 1.85 ppm were assigned to protons of CH_3 groups attached to isoxazole moiety. In conjugate LS-07, the singlet at δ 2.24 ppm was assigned to proton of CH_3 group attached to carbonyl group (acetyl group) of sulfonamide. In conjugate LS-05, the singlet at δ 2.45 ppm was assigned to proton of CH_3 group attached to pyrimidine moiety. In addition, all the other aliphatic and aromatic protons of all conjugates appeared at appropriate values of chemical shifts and integrals as explained in experimental section. In ^{13}C NMR spectra, conjugates LS01-LS09 exhibited the characteristics values of shifts at δ 146.35–144.75 ppm assigned to imine carbon (*-C = N-*). The carbonyl carbon all conjugates exhibited the signal between δ 166.71–164.20 ppm and carbonyl carbon of amide group was exhibited at δ 174.64 ppm. The signals for carbon of CH_3 groups attached to different moieties were obtained between δ 22.53, 18.39–18.35, 16.25 ppm for all conjugates. So, ^{13}C NMR spectral analyses were consistent with assigned structure of all compounds.

3.2. Urease inhibition

Indophenol method was employed for urease inhibition by newly synthesized Schiff bases after conjugation of levofloxacin with sulfa drugs. Serial dilution in range from 250–0.49 µM for each compound and levofloxacin was done for IC_{50} calculation (Table 1) whereas thiourea was used as standard inhibitor of urease. Compounds LS01 (IC_{50}= 0.58±0.11 µM), LS06 (IC_{50}= 0.45±0.21 µM) and LS07 (IC_{50}= 0.52±0.28 µM) were found to be more potent than levofloxacin (a well know urease inhibitor) and showed comparable activity against the jack bean urease. The compounds LS03-LS05 have pyrimidine with or without substitution of methyl group showed a bit high IC_{50} than LS06 in which pyrimidine attached to methoxy group (Table 1) whereas acetamide group attached to sulfoxide instead of pyrimidine also showed excellent antiurease activities.

Kinetic studies were performed for three most potent compounds LS01 (IC_{50}= 0.58±0.11 µM), LS06 (IC_{50}= 0.45±0.21 µM) and LS07 (IC_{50}= 0.52±0.28 µM) by varying their concentration (0–20 µM) along with different concentration of substrate (0.5–4.0 mM). Enzymatic kinetics determined the inhibition constant (K_i) and inhibition mode whether the inhibitors under investigation are competitive, mixed or non-competitive type. The effect of inhibitors (compounds) on V_{max} and K_m was determined to assess

Table 1
IC_{50} and kinetics parameters of newly designed Schiff bases.

Compound	IC_{50} (µM); mean±SEM (% inhibition)	[a]$V_{max\ (app)}$ (µM/min)	[b]$K_{m\ (app)}$ (mM)	[c]K_i (µM)	Mode of inhibition
LS01	0.58±0.11 (95.0)	0.70	1.44	3.40	Mixed
LS02	1.41±0.24 (93.9)	–	–	–	–
LS03	0.77±0.21 (94.0)	–	–	–	–
LS04	0.79±0.11 (95.0)	–	–	–	–
LS05	0.86±0.29 (93.2)	–	–	–	–
LS06	0.45±0.21 (91.1)	9.88	6.92	1.13	Competitive
LS07	0.52±0.28 (94.0)	3.16	1.30	6.03	Mixed
LS08	0.79±0.21 (95.5)				
LS09	1.65±1.21 (88.8)				
[d] Thiourea	15.51±0.11 (92.1)	18.61	2.18	18.18	Competitive
Levofloxacin	3.21±0.24 (91.0)	–	–	–	–

[a] Vmax (app)= Maximum velocity of enzymatic activity at 20 µM inhibitor concentration.
[b] Km(app)= Michaelis–Menten constant at 20 µM inhibitor concentration.
[c] Ki(µM)= Calculated from secondary Lineweaver Burk plot, d Standard inhibitor of urease.

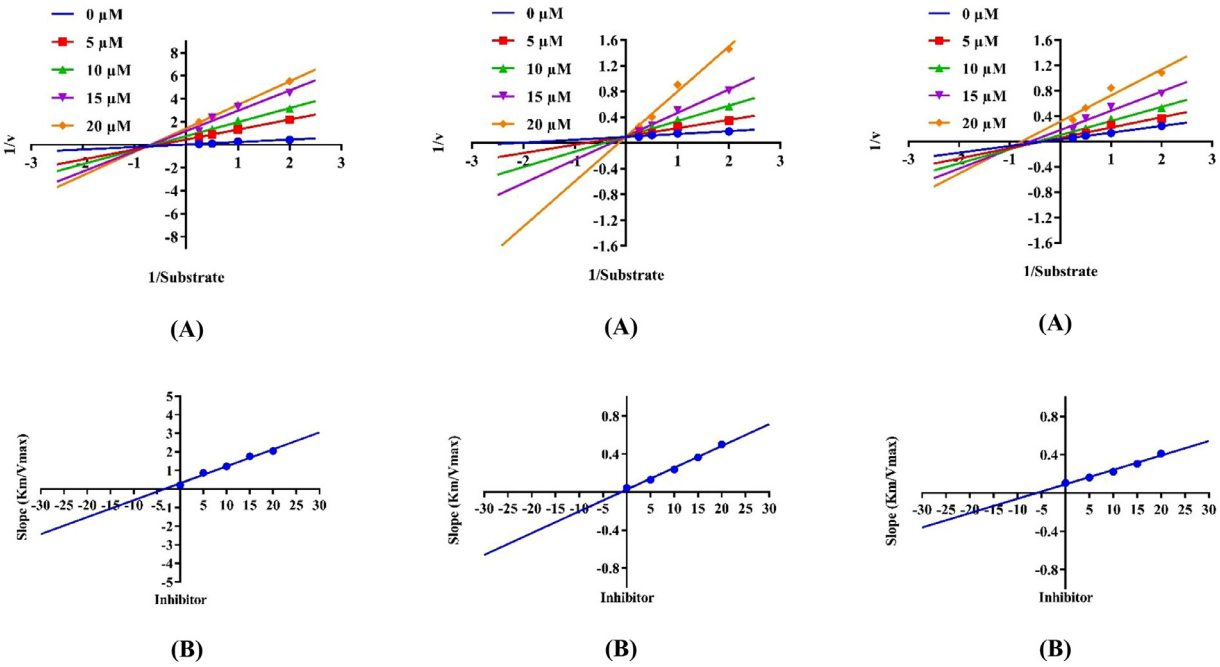

Fig. 2. Mode of inhibition exhibited by LS01, LS06 and LS07 explained by primary (A) and secondary (B) Lineweaver Burk plots.

the mode of inhibition by Lineweaver Burk plots. K_m of jack bean urease enzyme increases while V_{max} was not effected in the presence of LS06 which indicate the competitive mode of inhibition. V_{max} and K_m of urease enzyme were decreased and increased respectively in the presence of LS01 and LS07 which indicated that both the compounds showed the mixed type of inhibition these compounds could interact at the allosteric site or active site of the enzyme. Further inhibition constant (K_i) of each inhibitor (LS01, LS06 and LS07) was determined by secondary Lineweaver Burk plots. It was concluded from kinetic studies that compound LS06 was competitive inhibitor with Ki values (Table 1) 1.13 µM while the compounds LS01 and LS07were mixed type of inhibitors with Ki values 3.40 and 6.03 µM respectively (Table 1). The enzymatic kinetics of most active compounds is presented below in Fig. 2.

Sulfonamide derivatives serve as an important building blocks in the drug design, discovery and development process. Ciprofloxacin based sulfonamides [19] has been explored for antiurease activities and most potent compound (Fig. 1) revealed the IC_{50} value 0.045 µM with mixed type of mode of inhibition. Ciprofloxacin hydrazide and levofloxacin hydroxamic acid (Fig. 1) had shown the IC_{50} value 1.22 and 2.20 µM respectively and in this reported work no kinetic study was performed to access their binding mode [18]. Whereas in present work levofloxacin conjugated to sulfadoxine revealed the $IC_{50} = 0.45 \pm 0.21$ µM with competitive mode of inhibition.

3.3. Docking studies and ADMET properties calculations

After performing enzyme kinetic assays, the competitive inhibitor LS06 compound was docked at the catalytic site of the urease enzyme to predict its plausible binding mode. Fig 3A shows that compound has docked well in the binding pocket in which piperazine moiety is directed towards the Ni ion and making an electrostatic interaction. The carboxylate group present at three fused rings is making the ionic bridge with Arg-439 residue side chain. The substituted pyrimidine sulfonamide ring is spotted towards solvent exposed site of the binding site as shown in the surface model of protein ligand complex (Fig 3B). As docking score ranks the binding poses on the quality of interactions each pose is

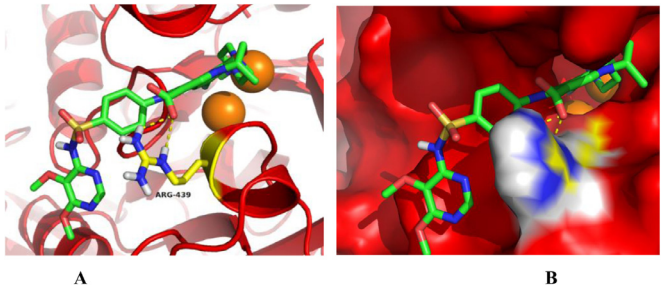

Fig. 3. Docking pose of the competitive inhibitor**: A)** Best docked pose of competitive inhibitor LS06 compound (green sticks) in urease enzyme catalytic site **B)** Surface representation of catalytic site with docked LS06 compound. Brown spheres are representing Ni ions whereas hydrogen bonding is shown with dotted yellow lines. Red color is the surface contour map of urease enzyme.

making with protein side chain, in our studies best binding mode shown in below mentioned figure yielded −4.77 kcal/mol.

Physiochemical/pharmacokinetic properties presented in Table 2 of all synthesized compounds were predicted using the Qikprop tool implemented in schrodinger software [35]. Most of the predicted values like water solubility, herg channel blockage, blood/brain barrier co-efficient, binding to human serum albumin and CNS values are within acceptable ranges except cell permeability of these compounds.

3.4. Computational studies

Synthesized compounds LS01-LS09 were initial optimized at method B3LYP with conjunction of 6–31G(d,p) basis set of DFT. The DFT based relaxed geometries (optimized geometries) are displayed in Fig. 4.

3.4.1. Frontier molecular orbital (FMO) analysis

Chemical stability, charge transfer, molecular interactions, electronic features and reactivity of good compounds are mostly inves-

Table 2
Calculated ADMET properties of newly designed Schiff bases.

ID	MW (g/mol)	HBD	HBA	QPlogPo/w	QPlogHERG	QPPCaco2 (nm/s)	QPlogBB	QPlogKhsa	CNS
LS01	610.659	2	13.25	1.521	−4.923	12.603	−1.329	0.17	−2
LS02	598.666	1	11.25	1.946	−5.083	12.588	−1.187	0.246	−2
LS03	593.631	2	13.75	1.021	−5.027	17.437	−1.024	−0.143	−2
LS04	607.658	2	13.75	1.265	−4.934	20.534	−1.006	−0.029	−2
LS05	621.685	2	13.75	1.547	−5.466	8.236	−1.690	0.185	−2
LS06	653.684	2	14.5	1.673	−5.746	10.499	−1.735	0.079	−2
LS07	557.595	2	12.25	0.663	−4.567	4.931	−1.609	0.014	−2
LS08	557.598	3	11.25	0.581	−4.664	1.902	−2.186	0.14	−2
LS09	515.558	3	11.75	0.124	−4.726	4.531	−1.695	−0.133	−2

MW = molecular weight,.
HBD = estimated no of hydrogen bond donor,.
HBA = estimated no of hydrogen bond acceptor,.
QPlogPo/*w* = Predicted octanol/water partition coefficient (recommended rage −2.0 to 6.5),.
CNS Predicted central nervous system activity on a –2 (inactive) to +2 (active) scale.
QPlogHERG = Predicted IC50 value for blockage of HERG K^+ channels (concern below <−5),.
QPCaco2 = Predicted Caco2 cell permeability in nm/*sec*. (recommended range < 25 poor, > 500 great),.
QPlogBB = Predicted brain/blood partition coefficient (recommended range −3.0 to 1.2),.
QPlogKhsa = Prediction of binding to human serum albumin (recommended range −1.5 to 1.5). [36].

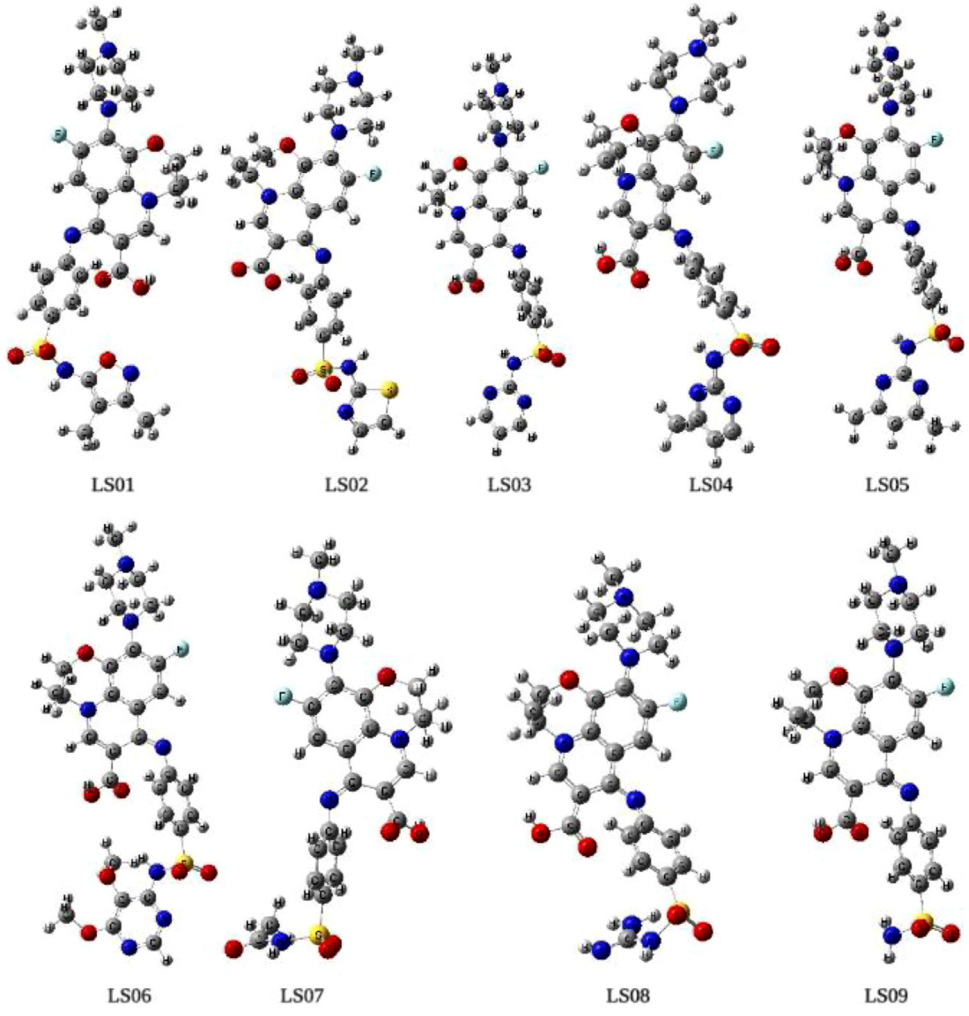

Fig. 4. Optimized geometries of synthesized compounds calculated at B3LYP/6–31 G (d,p) level of density functional theory.

tigated by doing frontier molecular orbitals analysis [37]. Moreover, mostly chemists and physicist also performed frontier molecular orbitals analysis for estimating the geometrical and structural characteristics of different compounds. Therefore we also used FMOs analysis to unveil the electron density donating and accepting ability of our compounds LS01-LS09. Both abilities i.e. electron density donating and accepting is estimated with the aid of band gap [38]. Chemical hardness, electron affinity, ionization potential with electronegativity, chemical potential and global chemical softness features of LS01-LS09 compounds LS01-LS09 compounds are also explored with aid of key band gap (i.e. HOMO-LUMO energy gap by using Eg=ELUMO-EHOMO). Narrow HOMO-LUMO gap grantees

Table 3
Frontier molecular orbitals (HOMO and LUMO) energies, energy gap (HOMO-LUMO gap) of studied compounds.

Compounds	E_{HOMO} (eV)	E_{LUMO} (eV)	E_g (eV)
LS01	−5.46	−1.61	3.84
LS02	−5.71	−1.99	3.72
LS03	−5.63	−1.76	3.87
LS04	−4.76	−1.77	2.99
LS05	−5.60	−1.73	3.87
LS06	−5.76	−1.89	3.87
LS07	−5.69	−1.84	3.85
LS08	−4.80	−2.09	2.31
LS09	−5.68	−1.71	3.97

a compound to be soft in nature with least stability and high reactivity whereas large value of HOMO-LUMO energy gap having compounds are marked as hard in nature with less reactivity and high stability. Alignment of FMOs (Frontier molecular orbitals) of all studied compounds LS01-LS09 were estimated at method B3LYP combined with basis set 6–31G(d,p)/DFT. Table 3 disclosed the computed results of FMOs.

The Eg values of investigated compounds LS01-LS09 are found between 2.31–3.97 eV. All compounds show similar Eg value with smaller difference. LS08 exhibited lowest HOMO-LUMO gap with a value of 2.31 eV and this might due to absence of any additional functional group whereas highest Eg is seen in the case of LS09 (Eg=3.97 eV) among all compounds. Finally, the DFT based computed energy band gap is examined as: LS08 < LS04 < LS02 < LS01 < LS07 < LS03=LS05=LS06 < LS09. Fig. 5 expressed the HOMO and LUMO charge distribution on molecules in which red color indicates negative charge density and similarly green color represents the presence of positive charge density.

3.4.2. Global reactivity descriptors

Information regarding chemical stability, charge transfer and chemical reactivity of LS01-LS09 is calculated with the aid of global indices of reactivity (details in supplementary data). HOMO-LUMO energies are played a key for estimation of above mentioned properties and the results are in Table 4.

Ionization potential and electron affinity values (Table 3) of LS01-LS09 indicates that our all compounds have electron donating potential as compared to electron accepting aptitude. Generally positive electron affinity values are seen in LS01-LS09 studied compounds which suggest that these compounds are suitable candidates for charge transfer reactions. As we earlier mentioned that these compounds are electron donating molecules in nature therefore the electron donor capability (ω-) of studied LS01-LS09 is larger as compare to electron accepting capability (ω+) and values in Table 3 supported our notation. Values of chemical softness (Table 4) of all studied compounds are very close to each other which suggest that studied compounds are potential candidates for biological applications with good softness values. A decreasing order for electronegativity values is observed in studied compound which is: LS02 > LS06 > LS09 > LS07 > LS03 > LS05 > LS01 > LS08 > LS04. Large value of global hardness is observed in all studied compounds which make the base of the chemically hard nature of these compounds. Large global hardness as compared to global softness of LS01-LS09 compounds indicated that these compounds are chemically stable with least reactivity. Chemical stability factor is also estimated with the aid of chemical potential μ values. Chemical potential μ has a direct concern with chemical stability and inverse concern with reactivity of specie. A descending order for chemical potential is observed in all studied compounds LS01-LS09 as: [LS02 (μ = −3.768 eV)] > [LS06 (μ = −3.741 eV)] > [LS09 (μ = −3.737 eV)] > [LS07 (μ = −3.709 eV)] >

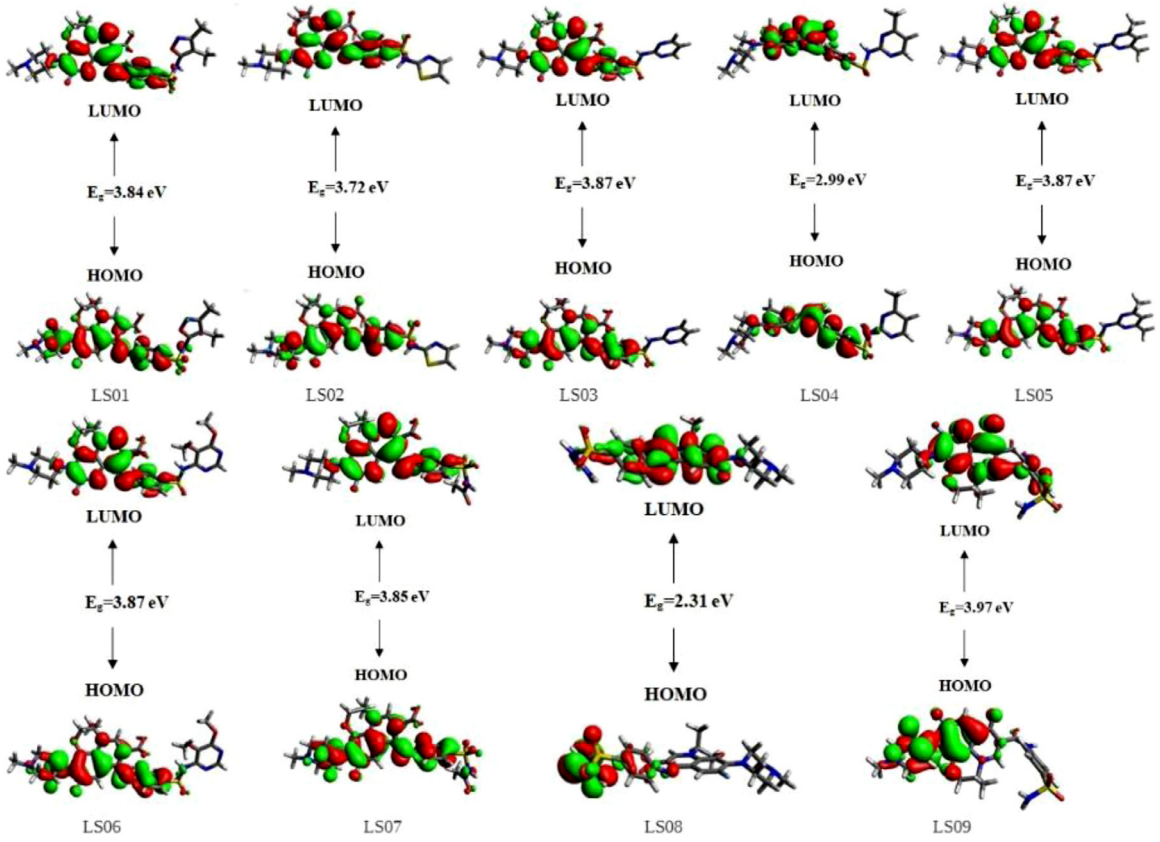

Fig. 5. Frontier molecular orbital (FMOs) representation of all studied compounds. Iso-surfaces value is 0.02e/Å3.

Table 4
Global electrophilicity (ω), electron donor capability (ω-), electron acceptor capability (ω+), global hardness (η), Ionization potential (I), electronegativity (χ), and global softness (σ), electron affinity (A) and chemical potential (μ).

	I (eV)	A (eV)	χ	H (eV)	μ (eV)	ω (eV)	ω-	ω+	σ (e/V)
LS01	6.604	0.337	3.471	3.134	−3.471	1.922	4.049	0.578	0.160
LS02	6.798	0.739	3.768	3.030	−3.768	2.344	4.606	0.838	0.165
LS03	6.813	0.481	3.647	3.166	−3.647	2.101	4.320	0.673	0.158
LS04	6.004	0.439	3.221	2.782	−3.221	1.865	3.823	0.602	0.180
LS05	6.763	0.448	3.606	3.157	−3.606	2.059	4.257	0.651	0.158
LS06	6.874	0.608	3.741	3.133	−3.741	2.234	4.496	0.755	0.160
LS07	6.867	0.550	3.709	3.158	−3.709	2.178	4.427	0.718	0.158
LS08	6.001	0.797	3.399	2.602	−3.399	2.221	4.245	0.846	0.192
LS09	7.112	0.363	3.737	3.374	−3.737	2.070	4.360	0.623	0.148

[LS03 (μ = −3.647 eV)] > [LS05 (μ = −3.606 eV)] > [LS01 (μ = −3.471 eV)] > [LS08 (μ = −3.399 eV)] > [LS04 (μ = −3.221 eV)]. From above order, it is clearly estimated that LS04 disclosed least value of chemical potential which mean that LS04 is least stable and reactive compounds among all studied compounds. This fact shows a good coherence with band gap order i.e. the molecule with narrow HOMO-LUMO energy gap exhibits high reactivity and very small kinetic stability with good softness value. In short, global indices of reactivity indicates that all studied compounds LS01-LS09 are stable in nature with good values of softness. In addition, all studied compounds disclosed electron donating behavior. Overall, all studied compounds are potential candidates for biological application and for charge transfer reactions.

3.4.3. Natural bond orbital (NBO) analysis

Non-covalent interaction along with hyper-conjugation in a compound is widely estimated with the aid of natural bonding orbital analysis. Intra-molecular hydrogen bonding originates within a compound due to presence of partial negative and partial positive charge atoms within is also investigated with the usage of NBO analysis. Moreover, the shifting of charge density from electron filled orbital (Lewis type NBOs orbitals) to electron empty orbital (Non-Lewis NBOs orbitals) is also estimated with the aid of natural bonding orbital analysis. So, motivated from all these finding we also make an attempt to unveil the characteristic regarding NBO analysis of LS01-LS09 compounds at method B3LYP combined with basis set 6–31 G(d,p)/DFT and computed results of these charge density shifting are enclosed in Table 1S. Eq. (1) helps in calculating the interactions and second order Fock Matrix.

$$E^2 = q_i \frac{(F_{i.j})^2}{\varepsilon_j - \varepsilon_i} \quad (1)$$

Here E2 stands for energy required for system stabilization, qi disclosed the occupancy of donor orbital, Fi,j expresses the elements of off diagonal NBO Fock matrix and describes diagonal elements. The results obtained from NBO analysis is tabulated (supplementary data Table 1S). Four different types of transition in a compound is observed by using natural bonding orbital analysis which are: $\sigma \rightarrow \sigma^*$, $\pi \rightarrow \pi^*$, L.P$\rightarrow\sigma^*$ and L.P$\rightarrow\pi^*$. Stabilization of compound is highly depends on intra-molecular hydrogen bonding which facilitates a lot regarding charge transfer. The confirmation of conjugation in a compound is estimated by $\pi \rightarrow \pi^*$ transition. The dominant $\pi \rightarrow \pi^*$ transitions in compounds LS01 is π (C27-C32) $\rightarrow$ π^* (C30-C31), in LS02 is π (C10-C11) $\rightarrow$ π^* (C24-C25), in LS03 is π (C40-C41) $\rightarrow$ π^* (N38-C29), in LS04 is π (C27-C28) $\rightarrow$ π^* (C29-C30), in LS05 is π (C27-C32) $\rightarrow$ π^* (C30-C31), in LS06 is π (C38-C39) $\rightarrow$ π^* (C37-N42), in LS07 is π (C27-

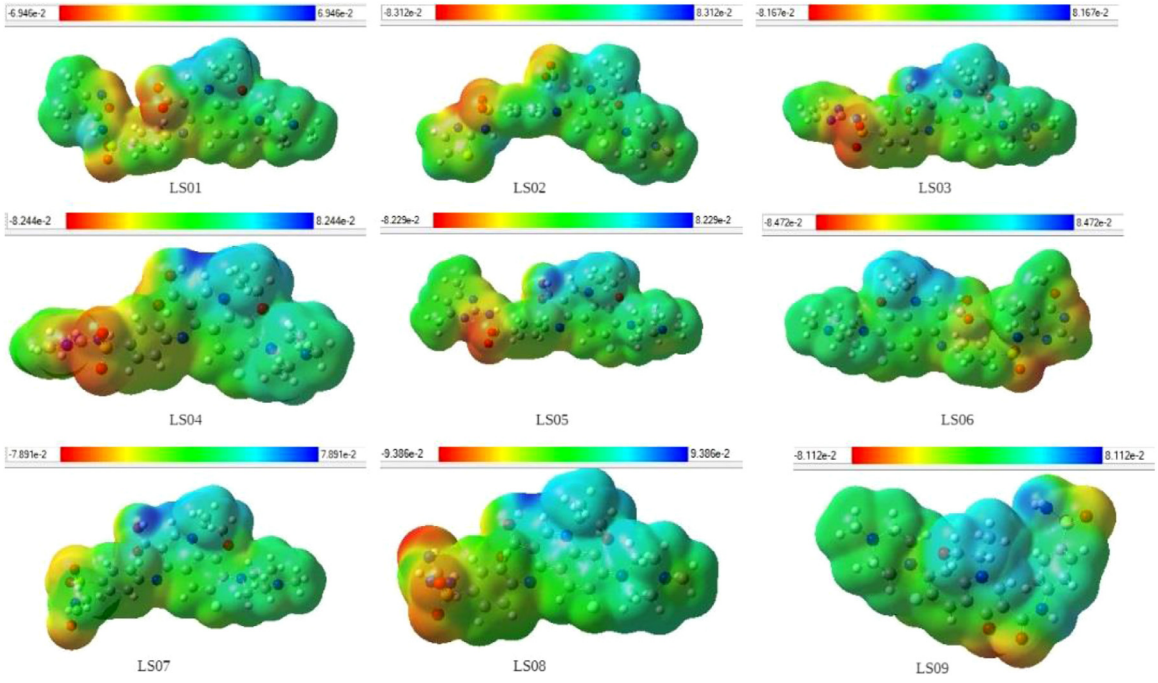

Fig. 6. DFT based computed MEP of all studied compounds at isosurfaces value is 0.02e/Å3.

C32) → π^* (C30-N31), in LS08 is π (C21-C22) → π^* (C10-C25) and in compound LS09 is π (C27-C28) → π^* (C27-C28) with stabilization energy of 28.46, 32.55, 34.94, 31.22, 28.03, 31.55, 28.02, 29.54 and 26.11 Kcal/mol respectively. Large values of stabilization energy in the case of resonance reveal that great delocalization of electron of oxygen or nitrogen bond to the entire system. These transitions are L.P (nitrogen) → π^* (carbon) in all compounds with stabilization energy of 46.55, 47.41, 47.12, 47.44, 46.99, 47.73, 47.02, 47.14 and 46.09 Kcal/mol for compounds LS01-LS09 respectively. The intra-molecular hydrogen bonding in all compounds is due to the delocalization of lone pair of nitrogen to π^* (pi anti-bonding orbital). In all compounds hydrogen bonding is present and it is intra-molecular in nature.

3.4.4. Molecular electrostatic potential (MEP) analysis

Molecular electrostatic potential (MEP) analysis aids in exploring the density plot on the whole compound. Eq. (2) helps in computing the molecular electrostatic potential in all target compounds.

$$V(r) = \sum(\frac{ZA}{RA} - r) - \int(p(r^{/})/r^{/} - r)dr^{/} \quad (2)$$

In above equation, V(r) is basically the MEP (molecular electrostatic potential) and ZA is used to indicate the presence of charge density over the nucleus. In addition, RA, p(r') is used to express the main electronic density function and similarly r' stands for the integration variable [39]. The sites for electrophilic and nucleophilic attack exhibit different color in MEP. Following increasing order is observed for electrostatic potential magnitude; red < orange < yellow < green < blue [40]. The red color is the preferable site for electrophilic attack and similarly blue color is the favorite site for nucleophilic attack. DFT/B3LYP/6–31 G (d,p) functionality is come into use for MEP analysis and results are portrayed in Fig. 5. In molecular electrostatic potential plot, the red color is due to oxygen atoms and blue color area is due to nitrogen, carbon and hydrogen atoms. Green area represents the mean potential area (the area between two extremes). From Fig. 6, it is cleared that different colors are presents on different atoms which suggest that different reactive sites are presents in all studied molecules.

4. Conclusion

In this study, nine Schiff bases were successfully synthesized, physiochemical and spectral analysis were performed to confirm their structures. The compounds were screened for antiurease activities and among the tested compounds, LS06 exhibited lowest IC_{50} value (0.45±0.21 µM). Primary and secondary Lineweaver Burk plots were drawn to assess the inhibition mechanism, LS06 showed the competitive mode of inhibition while LS01 and LS07 revealed mixed type of inhibition. Insights of DFT study of these compounds unveil their good stability by using different analysis like natural bonding analysis, global indices of reactivity and molecular electrostatic potential analysis.

Author statement

Syed Azhar Ali Shah Tirmazi: Methodology, Writing - original draft. Muhammad Abdul Qadir: Supervision. Mahmood Ahmed: Investigation, Methodology, Formal analysis, Writing - original draft. Biological assays, Kinetic studies, Muhammad Imran: Writing - original draft. Biological assays, kinetic assays, Mehwish Sharif: DFT data review, Muhammad Yousaf: Spectroscopic data analysis, Muhammad Muddassar: Molecular docking, Riaz Hussain: DFT calculation,

Compliance with ethical standards

Informed consent: Not applicable

Declaration of Competing Interest

We wish to confirm that there are no known conflicts of interest associated with this publication.

Funding Agency

There has been no financial support for this work that could have influenced its outcome.

Acknowledgement

The authors would like to thank Higher Education Commission of Pakistan for providing financial support to purchase software licenses and hardware for *in silico* studies vide Projects No. 6804/Federal/NRPU/R&D/HEC/ 2016 & 8094/Balochistan/NRPU/R&D/HEC/2017.

Supplementary materials

Supplementary material associated with this article can be found, in the online version, at doi:10.1016/j.molstruc.2021.130226.

References

[1] A. Hameed, K.M. Khan, S.T. Zehra, R. Ahmed, Z. Shafiq, S.M. Bakht, M. Yaqub, M. Hussain, A.d.l.V. de León, N. Furtmann, Synthesis, biological evaluation and molecular docking of N-phenyl thiosemicarbazones as urease inhibitors, Bioorg. Chem. 61 (2015) 51–57.
[2] W.-.K. Shi, R.-.C. Deng, P.-.F. Wang, Q.-.Q. Yue, Q. Liu, K.-.L. Ding, M.-.H. Yang, H.-.Y. Zhang, S.-.H. Gong, M. Deng, 3-Arylpropionylhydroxamic acid derivatives as Helicobacter pylori urease inhibitors: synthesis, molecular docking and biological evaluation, Bioorg. Med. Chem. 24 (2016) 4519–4527.
[3] H. Mobley, M.D. Island, R.P. Hausinger, Molecular biology of microbial ureases, Microbiology and Molecular Biology Reviews 59 (1995) 451–480.
[4] K. Stingl, K. Altendorf, E.P. Bakker, Acid survival of Helicobacter pylori: how does urease activity trigger cytoplasmic pH homeostasis? Trends Microbiol. 10 (2002) 70–74.
[5] P. Krishnamurthy, M. Parlow, J.B. Zitzer, N.B. Vakil, H.L. Mobley, M. Levy, S.H. Phadnis, B.E. Dunn, Helicobacter pylori containing only cytoplasmic urease is susceptible to acid, Infect. Immun. 66 (1998) 5060–5066.
[6] M.W. Pinkse, C.S. Maier, J.I. Kim, B.H. Oh, A.J. Heck, Macromolecular assembly of Helicobacter pylori urease investigated by mass spectrometry, Journal of Mass Spectrometry 38 (2003) 315–320.
[7] D.J. Evans Jr, D.G. Evans, S.S. Kirkpatrick, D.Y. Graham, Characterization of the Helicobacter pylori urease and purification of its subunits, Microb. Pathog. 10 (1991) 15–26.
[8] P. Kosikowska, Ł. Berlicki, Urease inhibitors as potential drugs for gastric and urinary tract infections: a patent review, Expert Opin Ther Pat 21 (2011) 945–957.
[9] A. Rauf, S. Shahzad, M. Bajda, M. Yar, F. Ahmed, N. Hussain, M.N. Akhtar, A. Khan, J. Jończyk, Design and synthesis of new barbituric-and thiobarbituric acid derivatives as potent urease inhibitors: structure activity relationship and molecular modeling studies, Bioorg. Med. Chem. 23 (2015) 6049–6058.
[10] Y. Gull, N. Rasool, M. Noreen, A. Altaf, S. Musharraf, M. Zubair, F.-U.-H. Nasim, A. Yaqoob, V. DeFeo, M. Zia-Ul-Haq, Synthesis of N-(6-Arylbenzo [d] thiazole-2-acetamide derivatives and their biological activities: an experimental and computational approach, Molecules 21 (2016) 266.
[11] L.V. Modolo, A.X. de Souza, L.P. Horta, D.P. Araujo, A. de Fatima, An overview on the potential of natural products as ureases inhibitors: a review, J Adv Res. 6 (2015) 35–44.
[12] P. Przybylski, A. Huczynski, K. Pyta, B. Brzezinski, F. Bartl, Biological properties of Schiff bases and azo derivatives of phenols, Curr Org Chem. 13 (2009) 124–148.
[13] M. Ahmed, M.A. Qadir, M.I. Shafiq, M. Muddassar, Z.Q. Samra, A. Hameed, Synthesis, characterization, biological activities and molecular modeling of Schiff bases of benzene sulfonamides bearing curcumin scaffold, Arab. J. Chem. 12 (2019) 41–53.
[14] A.O.d. Souza, F. Galetti, C.L. Silva, B. Bicalho, M.M. Parma, S.F. Fonseca, A.J. Marsaioli, A.C. Trindade, R.P.F. Gil, F.S. Bezerra, Antimycobacterial and cytotoxicity activity of synthetic and natural compounds, Quím. Nova. 30 (2007) 1563–1566.

[15] Z. Guo, R. Xing, S. Liu, Z. Zhong, X. Ji, L. Wang, P. Li, Antifungal properties of Schiff bases of chitosan, N-substituted chitosan and quaternized chitosan, Carbohydr. Res. 342 (2007) 1329–1332.
[16] R.A. Nadeem, M. Abdul Qadir, M. Ahmed, I. Sajid, Cephalosporin conjugated sulfonamides: synthesis, characterization and anticancer activities, Lett Drug Des Discov 17 (2020) 264–270.
[17] M. Ahmed, M.A. Qadir, S. Ahmad, I. ul-Huq, R. Hussain, T. Habib, R. Ikram, M. Muddassar, Studies on the synthesis of benzene sulfonamides, evaluation of their antimicrobial activities, and molecular docking, Lat. Am. J. Pharm. 39 (2020) 38–46.
[18] M.A. Abdullah, G.E.-D.A. Abuo-Rahma, E.-S.M. Abdelhafez, H.A. Hassan, R.M.A. El-Baky, Design, synthesis, molecular docking, anti-Proteus mirabilis and urease inhibition of new fluoroquinolone carboxylic acid derivatives, Bioorg. Chem. 70 (2017) 1–11.
[19] P.A. Channar, A. Saeed, F. Albericio, F.A. Larik, Q. Abbas, M. Hassan, H. Raza, S.-Y. Seo, Sulfonamide-linked ciprofloxacin, sulfadiazine and amantadine derivatives as a novel class of inhibitors of Jack bean urease; synthesis, kinetic mechanism and molecular docking, Molecules 22 (2017) 1352.
[20] M. Taha, N.H. Ismail, M.S. Baharudin, S. Lalani, S. Mehboob, K.M. Khan, S. Siddiqui, F. Rahim, M.I. Choudhary, Synthesis crystal structure of 2-methoxybenzoylhydrazones and evaluation of their α-glucosidase and urease inhibition potential, Med. Chem. Res. 24 (2015) 1310–1324.
[21] I. Anis, M. Aslam, N. Afza, A. Hussain, F. Ahmad, L. Iqbal, M. Lateef, M. Hussain, T. Bokhari, A one-pot synthesis, characterization and pharmacological investigations: schiff bases, IJPC (2012).
[22] M. Taha, N.H. Ismail, A. Khan, S.A.A. Shah, A. Anwar, S.A. Halim, M.Q. Fatmi, S. Imran, F. Rahim, K.M. Khan, Synthesis of novel derivatives of oxindole, their urease inhibition and molecular docking studies, Bioorg. Med. Chem. Lett. 25 (2015) 3285–3289.
[23] S. Imran, M. Taha, N. Ismail, K. Khan, F. Naz, M. Hussain, S. Tauseef, Synthesis of novel bisindolylmethane Schiff bases and their antibacterial activity, Molecules 19 (2014) 11722–11740.
[24] M. Ahmed, M.A. Qadir, A. Hameed, M.N. Arshad, A.M. Asiri, M. Muddassar, Azomethines, isoxazole, N-substituted pyrazoles and pyrimidine containing curcumin derivatives: urease inhibition and molecular modeling studies, Biochem. Biophys. Res. Commun. 490 (2017) 434–440.
[25] H.J. Benson, Microbiological Applications: Laboratory Manual in General Microbiology, McGraw-Hill, 2002.
[26] M.A. Abdullah, R.M.A. El-Baky, H.A. Hassan, E.-S.M. Abdelhafez, G.E.-D.A. Abuo-Rahma, Fluoroquinolones as urease inhibitors: anti-proteus mirabilis activity and molecular docking studies, Am. J. Microbiol. Res. 4 (2016) 81–84.
[27] I. Nishimori, T. Minakuchi, T. Kohsaki, S. Onishi, H. Takeuchi, D. Vullo, A. Scozzafava, C.T. Supuran, Carbonic anhydrase inhibitors: the β-carbonic anhydrase from Helicobacter pylori is a new target for sulfonamide and sulfamate inhibitors, Bioorg. Med. Chem. Lett. 17 (2007) 3585–3594.
[28] T. Tanaka, M. Kawase, S. Tani, Urease inhibitory activity of simple α, β-unsaturated ketones, Life Sci. 73 (2003) 2985–2990.
[29] M. Imran, S. Waqar, K. Ogata, M. Ahmed, Z. Noreen, S. Javed, N. Bibi, H. Bokhari, A. Amjad, M. Muddassar, Identification of novel bacterial urease inhibitors through molecular shape and structure based virtual screening approaches, RSC Adv 10 (2020) 16061–16070.
[30] M. Ahmed, M. Imran, M. Muddassar, R. Hussain, M.U. Khan, S. Ahmad, M.Y. Mehboob, S. Ashfaq, Benzenesulfonohydrazides inhibiting urease: design, synthesis, their in vitro and in silico studies, J. Mol. Struct. 1220 (2020) 128740.
[31] M. Frisch, G. Trucks, H. Schlegel, G. Scuseria, M. Robb, J. Cheeseman, G. Scalmani, V. Barone, B. Mennucci, G. Petersson, Gaussian09 Revision D. 01, Gaussian Inc, Wallingford CT, 2009 See also: URL http://www.gaussian.com DOI.
[32] R. Dennington, T. Keith, J.G. Millam, Version 5, Semichem Inc, 2009 Shawnee Mission, KS, DOI.
[33] M.D. Hanwell, D.E. Curtis, D.C. Lonie, T. Vandermeersch, E. Zurek, G.R. Hutchison, Avogadro: an advanced semantic chemical editor, visualization, and analysis platform, J Cheminform 4 (2012) 17.
[34] G.A. Andrienko, Chemcraft. Graphical software for visualization of quantum chemistry computations, 2010.
[35] S. Release, 2: LigPrep, Schrödinger (2017) New York, NY, DOI (2017).
[36] A. Tahir, R.D. Alharthy, S. Naseem, N. Mahmood, M. Ahmed, K. Shahzad, M.N. Akhtar, A. Hameed, I. Sadiq, H. Nawaz, M. Muddassar, Investigations of structural requirements for brd4 inhibitors through ligand- and structure-based 3D QSAR approaches, Molecules 23 (2018).
[37] M. Srnec, E.I. Solomon, Frontier molecular orbital contributions to chlorination versus hydroxylation selectivity in the non-heme iron halogenase SyrB2, J. Am. Chem. Soc. 139 (2017) 2396–2407.
[38] S. Hussain, S.A.S. Chatha, A.I. Hussain, R. Hussain, M.Y. Mehboob, S. Muhammad, Z. Ahmad, K. Ayub, Zinc-Doped Boron Phosphide Nanocluster as Efficient Sensor for SO2, J Chem (2020) 12 2020.
[39] S. Muthu, A. Prabhakaran, Vibrational spectroscopic study and NBO analysis on tranexamic acid using DFT method, Spectrochimica. Acta Part A: Mol. Biomol. Spectroscopy 129 (2014) 184–192.
[40] G. Mahalakshmi, V. Balachandran, NBO, HOMO, LUMO analysis and vibrational spectra (FTIR and FT Raman) of 1-Amino 4-methylpiperazine using ab initio HF and DFT methods, Spectrochimica Acta Part A: Mol. Biomol. Spectroscopy 135 (2015) 321–334.